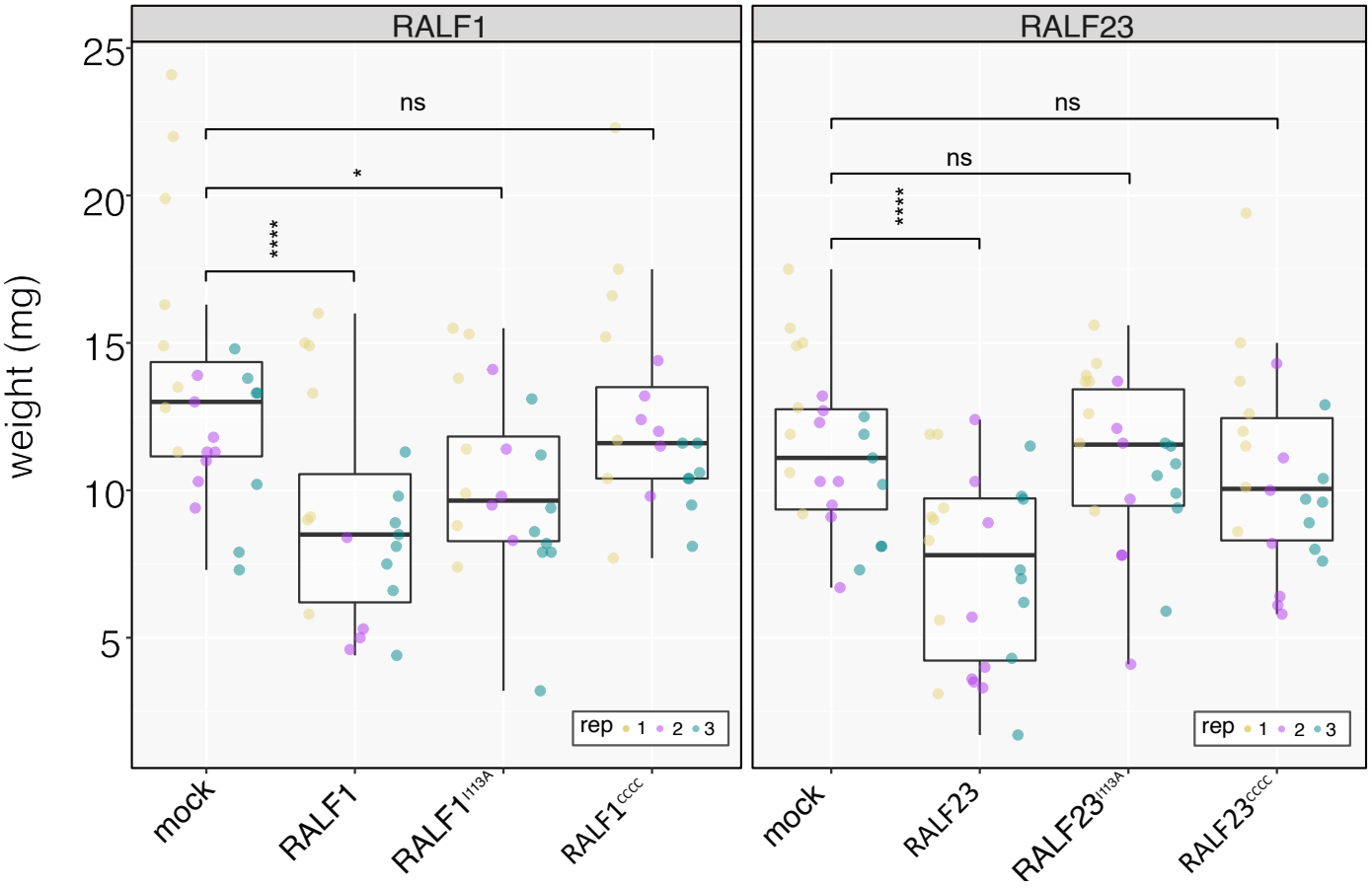

Supplemental Figure S1. YISY motif and conserved cysteine residues are important for *At*RALF bioactivity. Fresh weight of 12-day-old seedlings grown in the absence (mock) or presence of 10 μM RALF peptides (n=8). Data from three independent repetitions are shown (colours indicate different replicates). Upper and lower whiskers represent 1.5 times and −1.5 times interquartile range; upper and lower hinges represent 25 % and 75 % quartiles; middle represents median or 50 % quartile. Asterisks indicate significance levels of a one-way ANOVA followed by a Dunnet test comparing each treatment to the mock treatment: ns (p-value >0.05), * (p-value ≤ 0.05) and **** (p-value ≤ 0.0001).

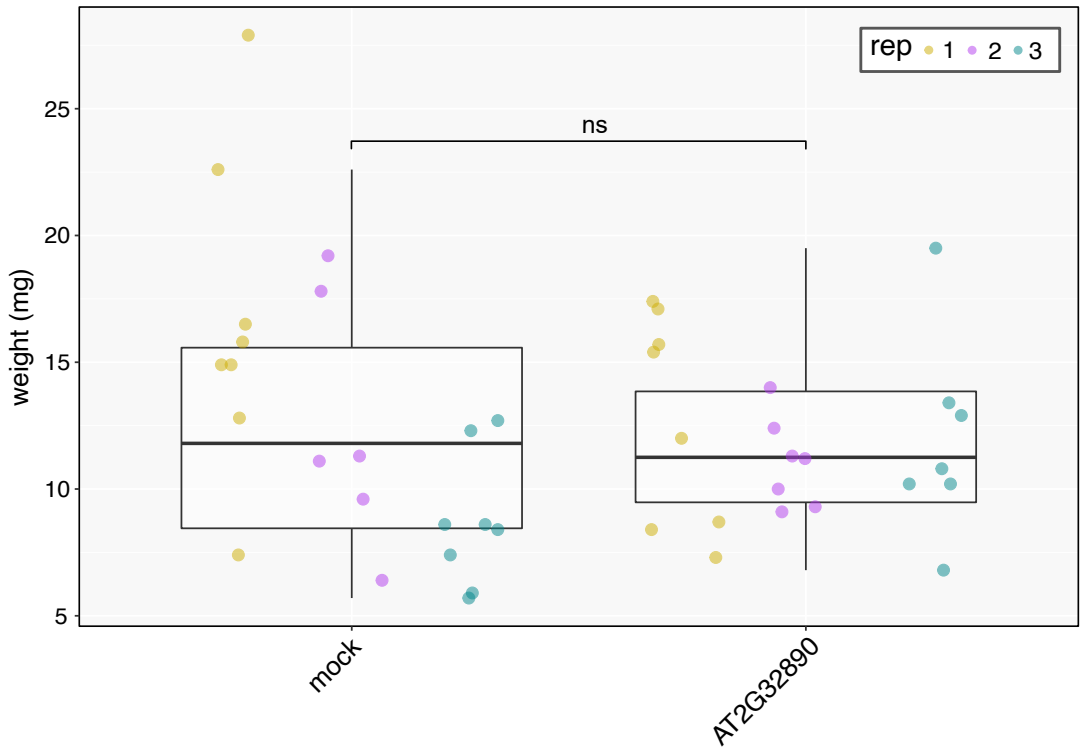

Supplemental Figure S2. Fresh weight of 12-day-old seedings grown in the absence (mock) or presence of 10 μM AT2G32890 peptide (n=8). Data from three independent repetitions are shown (colours indicate different replicates). Upper and lower whiskers represent 1.5 times and -1.5 times interquartile range; upper and lower hinges represent 25 % and 75 % quartiles; middle represents median or 50 % quartile. Asterisks indicate significance levels of a Kruskal-Wallis' multiple comparison test; each treatment was compared to their corresponding mock treatment: ns (p-value > 0.05).

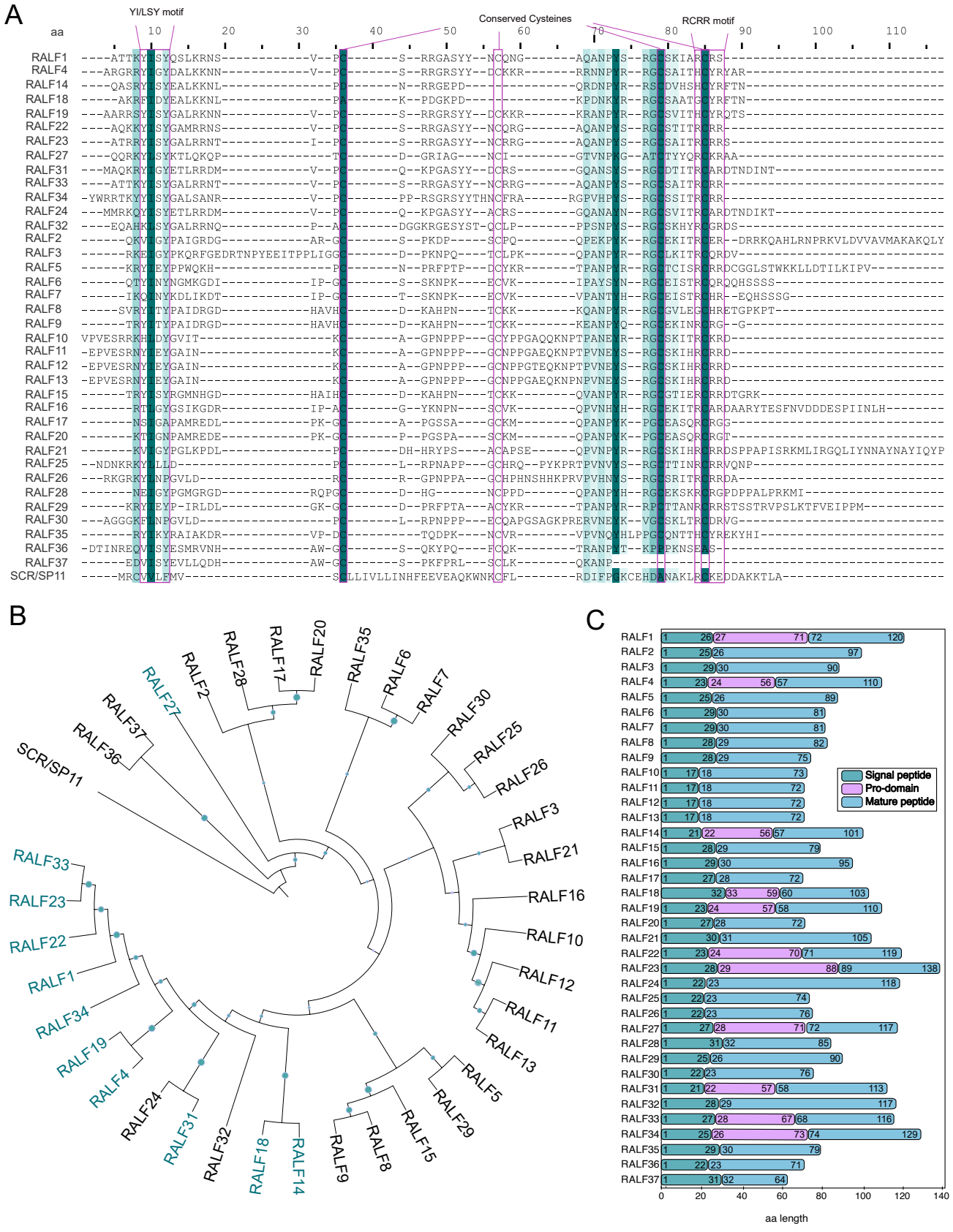

Supplemental Figure S3. Phylogenetic relationship of our proposed revised consensus list of *At*RALF. (A) Alignment of the C-terminal part of consensus *At*RALF peptides. Colour-code based on sequence conservation. The darker the colour, the more conserved the residue. Pink boxes indicate conserved motifs. (B) Phylogenetic rooted tree of the *At*RALF peptides. UPGMA tree inferred from the MUSCLE alignment displayed in (A) S-locus protein 11 or S-locus Cys-rich (SCR/SP11) sequence was used to root the tree. RALFs highlighted in teal indicated those predicted to be cleaved by the protease S1P. Bootstrap values (1000 repetitions) above 50 % are represented by green circles in the corresponding branches. The higher the bootstrap value for a particular branch, the higher the size of the circle (C) Schematic representation of *A. thaliana* PRORALFs domains. RALF peptides are expressed as protein precursors that require further processing steps. They contain an N-terminal SP (in green), variable pro domain for those that are predicted to be cleaved (pink) and a mature C-terminal part (blue).

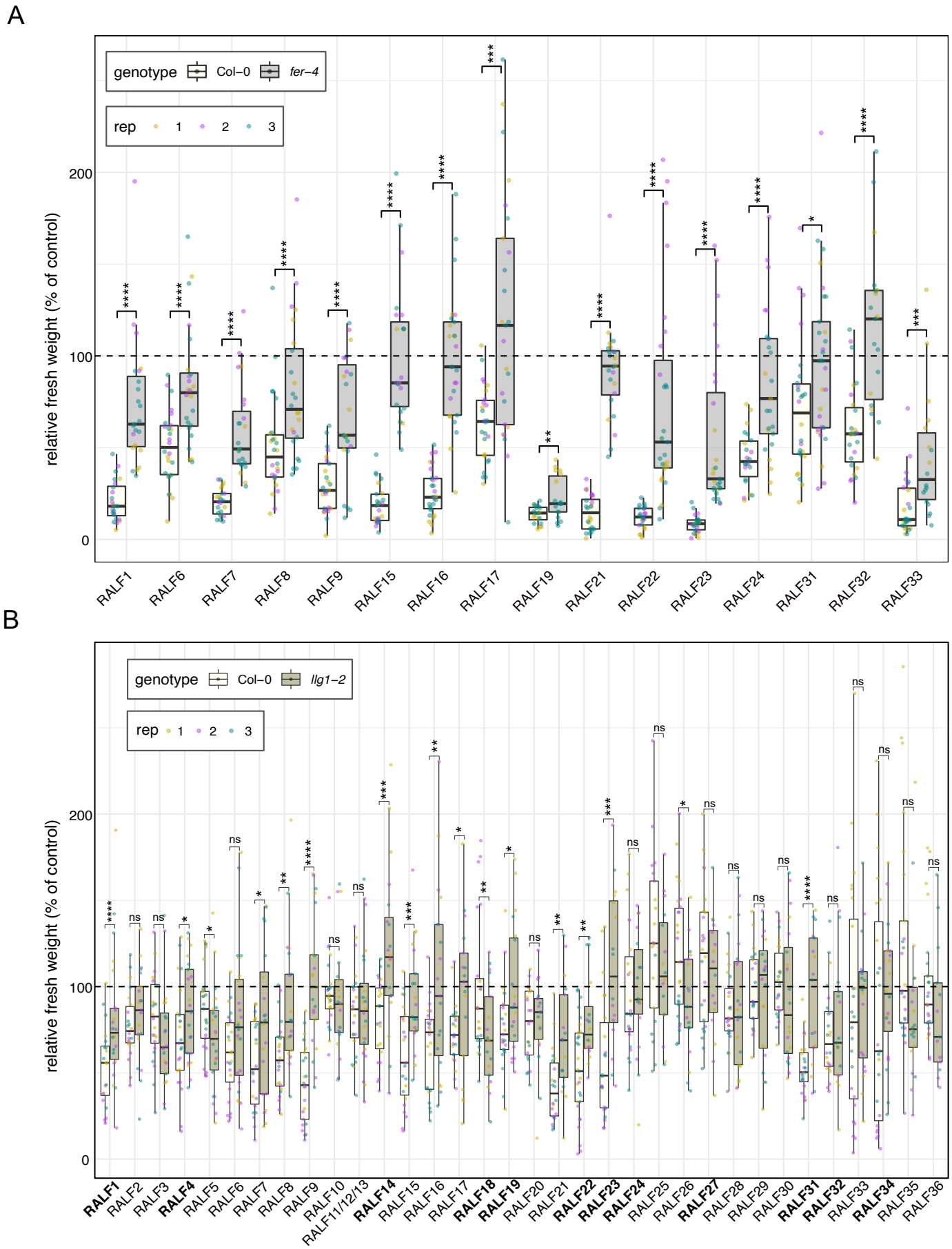

Supplemental Figure S4. FER-dependency of *At*RALF peptides in inducing seedling growth inhibition at 10 μM. (A) Fresh weight of 12-day-old seedlings grown in the presence of 10 μM RALF peptides relative to mock. RALF peptides that were active at 1 μM in seedling growth inhibition assays in Col-0 and FER-dependent were used. Mock treatment of Col-0 (white) and *fer-4* (grey) correspond to 100 % in the y axis. (B) Fresh weight of 12-day-old seedlings grown in the presence of 2 μM RALF peptides relative to mock treatment. Mock-treated seedlings weight of Col-0 (white) and *llg1-2* (green) correspond to 100 % in the y axis. RALF peptides indicated in bold correspond to predicted LLG1- dependent RALFs. A and B, Data from three independent repetitions are shown (colours indicate different replicates). Upper and lower whiskers represent 1.5 times and −1.5 times interquartile range; upper and lower hinges represent 25 % and 75 % quartiles; middle represents median or 50 % quartile. Asterisks indicate significance levels of a two-tailed T-test comparing each treatment in *fer-4* or *llg1-2* to the corresponding treatment in Col-0: ns (p-value >0.05), * (p-value ≤ 0.05), ** (p-value ≤ 0.01), *** (p-value ≤ 0.001) and **** (p-value ≤ 0.0001).

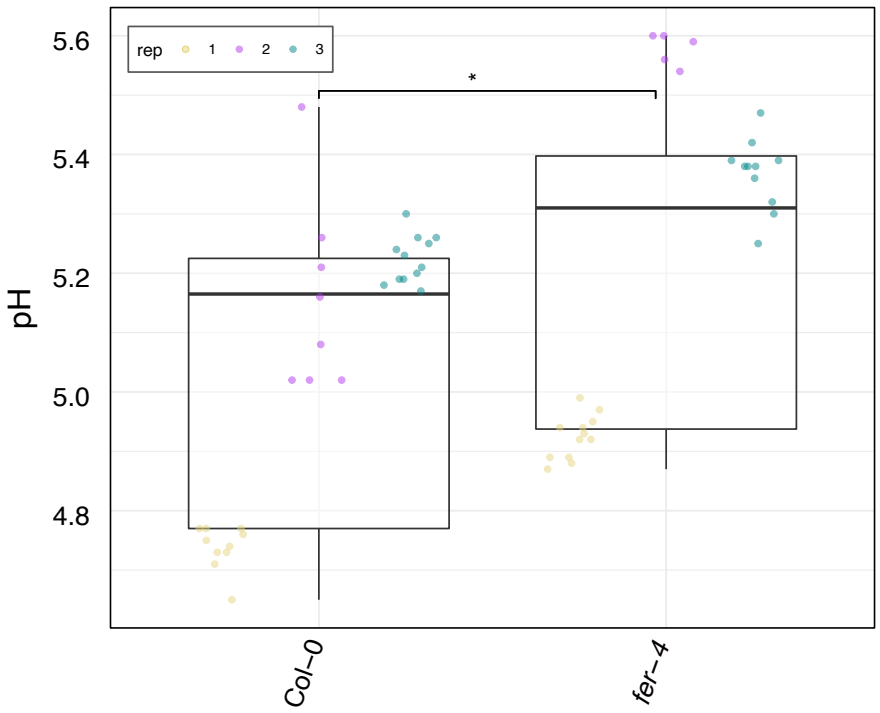

Supplemental Figure S5. *fer-4* bathing medium is more alkaline than Col-0 medium. pH values of 7-day-old Col-0 and *fer-4* seedlings recorded 4 hours after transferring seedlings into liquid MS with no treatment
(mock). Data from three independent repetitions are shown (colours indicate different replicates). Asterisk indicates significance levels of a two-tailed t-test: * (p-value ≤ 0.05). Upper and lower whiskers represent 1.5 times and −1.5 times interquartile range; upper and lower hinges represent 25 % and 75 % quartiles; middle represents median or 50 % quartile.

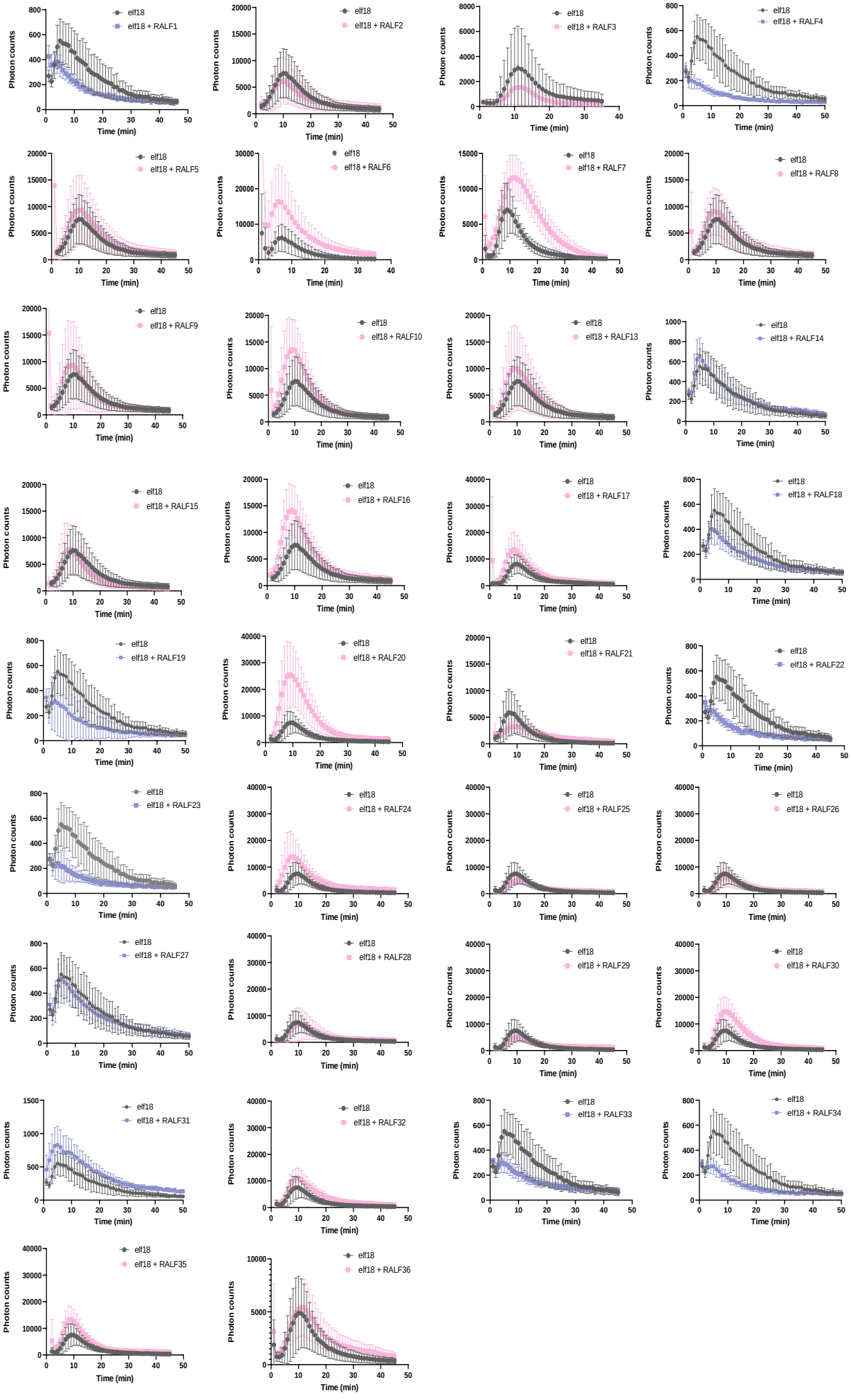

Supplemental Figure S6. Effect of *At*RALF peptides on elf18-induced ROS production. ROS production in Col-0 leaf discs co-treated with 100 nM elf18 and 1 µM RALF peptides or elf18 alone as control. Shown are the kinetics of one representative replicate. Predicted S1P-cleaved RALF peptides are indicated in blue and non-cleaved in pink.

A

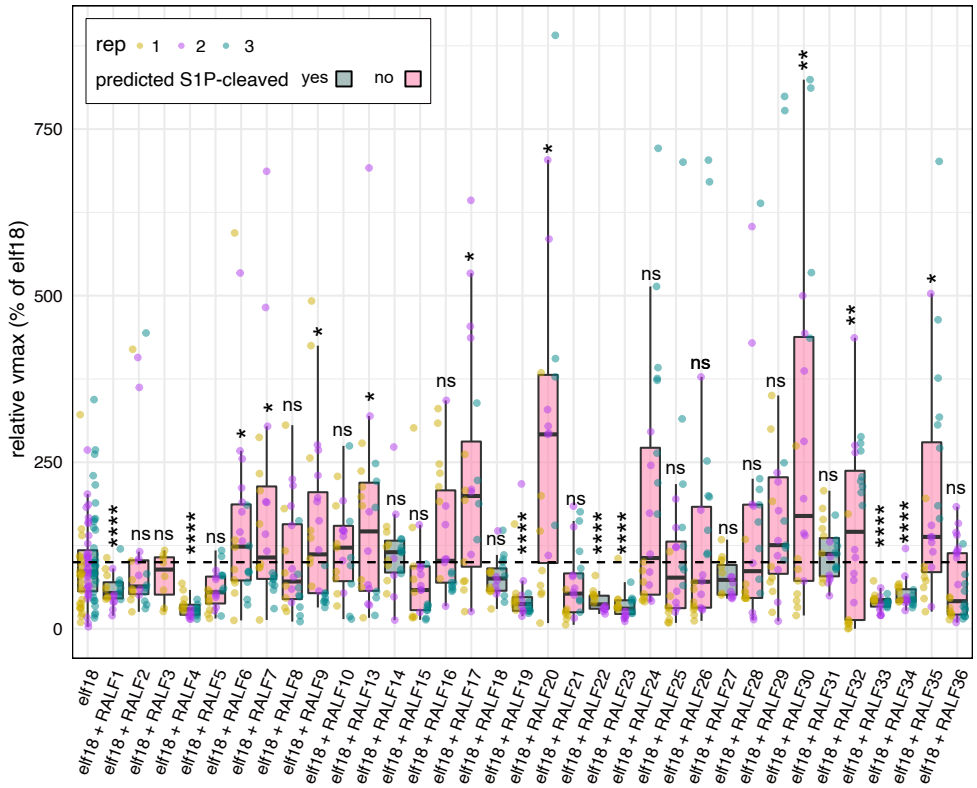

B

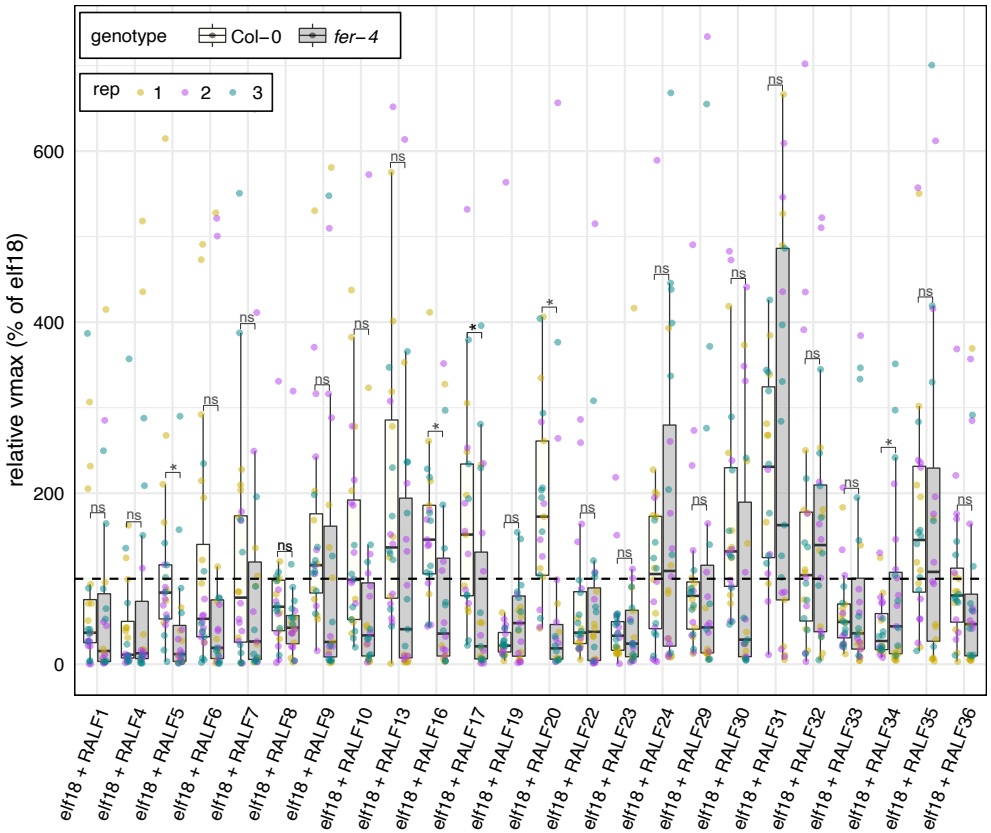

Supplemental Figure S7. Effect of *At*RALF peptides on ROS production. (A) ROS production in Col-0 leaf discs co-treated with 100 nM elf18 and 1 μM RALF peptides. In blue, box-plots of predicted S1P-cleaved RALF peptides and in pink, box-plots of non-cleaved RALF peptides. Asterisks indicate significance levels of a one-way ANOVA followed by a Dunnet test comparing each treatment to elf18 (B) ROS production in Col-0 and *fer-4* leaf discs co-treated with 100 nM elf18 and 1 μM RALF peptides. Col-0 data are shown in white and *fer-4* data in grey. Asterisks indicate significance levels of a two-tailed T-test comparing each treatment in *fer-4* to the corresponding in Col-0. A and B, Maximal velocity (vmax) values of the ROS curves relative to elf18 data are shown, n = 8. elf18 ROS data correspond to 100 % (dashed lines) in the y axis. Upper and lower whiskers represent 1.5 times and −1.5 times interquartile range; upper and lower hinges represent 25 % and 75 % quartiles; middle represents median or 50 % quartile. Data from three independent repetitions are shown (colours indicate different replicates). Asterisk significance: ns (p-value >0.05), ** (p-value ≤ 0.01), *** (p-value ≤ 0.001) and **** (p-value ≤ 0.0001).

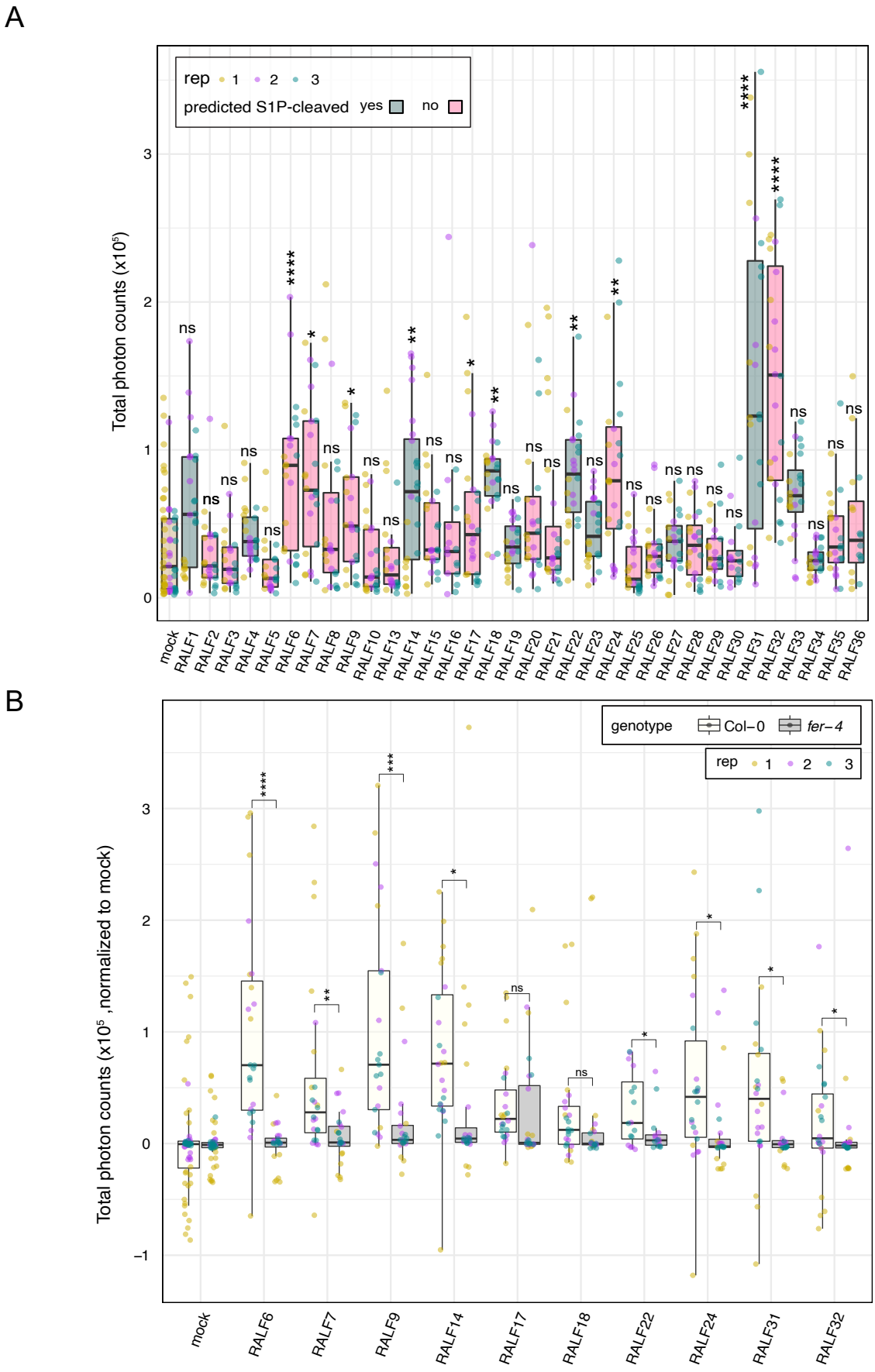

Supplemental Figure S8. Effect of *At*RALF peptides on ROS production in Col-0 and *fer-4*. (A) ROS production in Col-0 leaf discs treated with 1 μM RALF peptides. In blue, box-plots of predicted S1P-cleaved RALF peptides and in pink, box plots of non-cleaved RALF peptides. Asterisks indicate significance levels of a one-way ANOVA followed by a Dunnet test comparing each treatment to mock. Integration as mean values of total photon counts over 45 min ± SE, n = 8. (B) ROS production in Col-0 and *fer-4* leaf discs treated with 1 μM RALF peptides (n=8). Col-0 data are shown in white and *fer-4* data in grey. Asterisks indicate significance levels of a two-tailed T-test comparing each treatment in *fer-4* to the corresponding in Col-0. A and B, values are means of total photon counts over 45 min relative to mock data. Data from three independent repetitions are shown (colours indicate different replicates). Upper and lower whiskers represent 1.5 times and −1.5 times interquartile range; upper and lower hinges represent 25 % and 75 % quartiles; middle represents median or 50 % quartile. Asterisk significance: ns (p-value >0.05), ** (p-value ≤ 0.01), *** (p-value ≤ 0.001) and **** (p-value ≤ 0.0001).

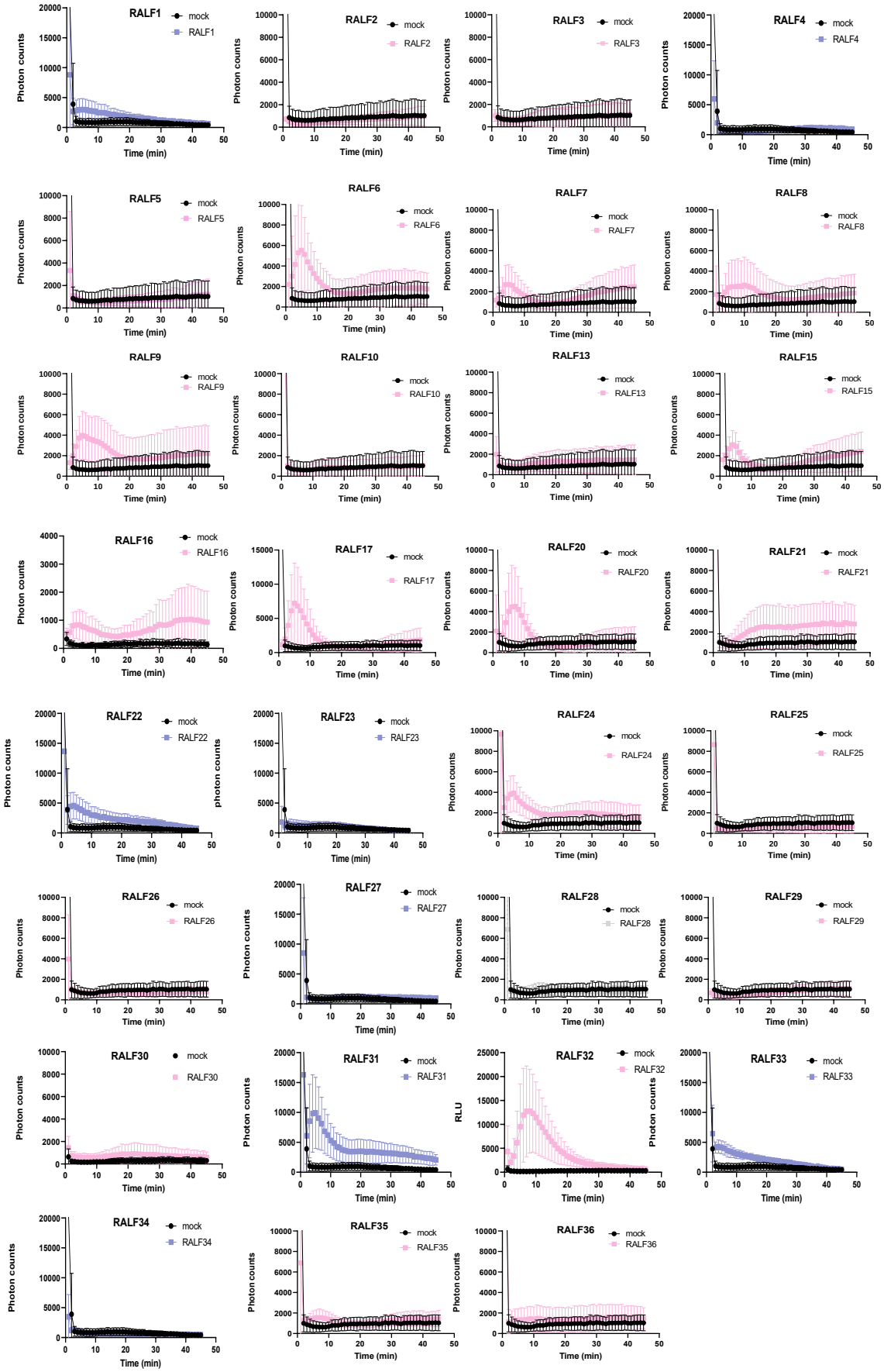

Supplemental Figure S9. Effect of *At*RALF peptides on ROS production. ROS production in Col-0 leaf discs treated with 1 uM RALF peptides. Shown are the kinetics of one representative replicate. Predicted S1P-cleaved RALF peptides are indicated in blue and non-cleaved in pink.

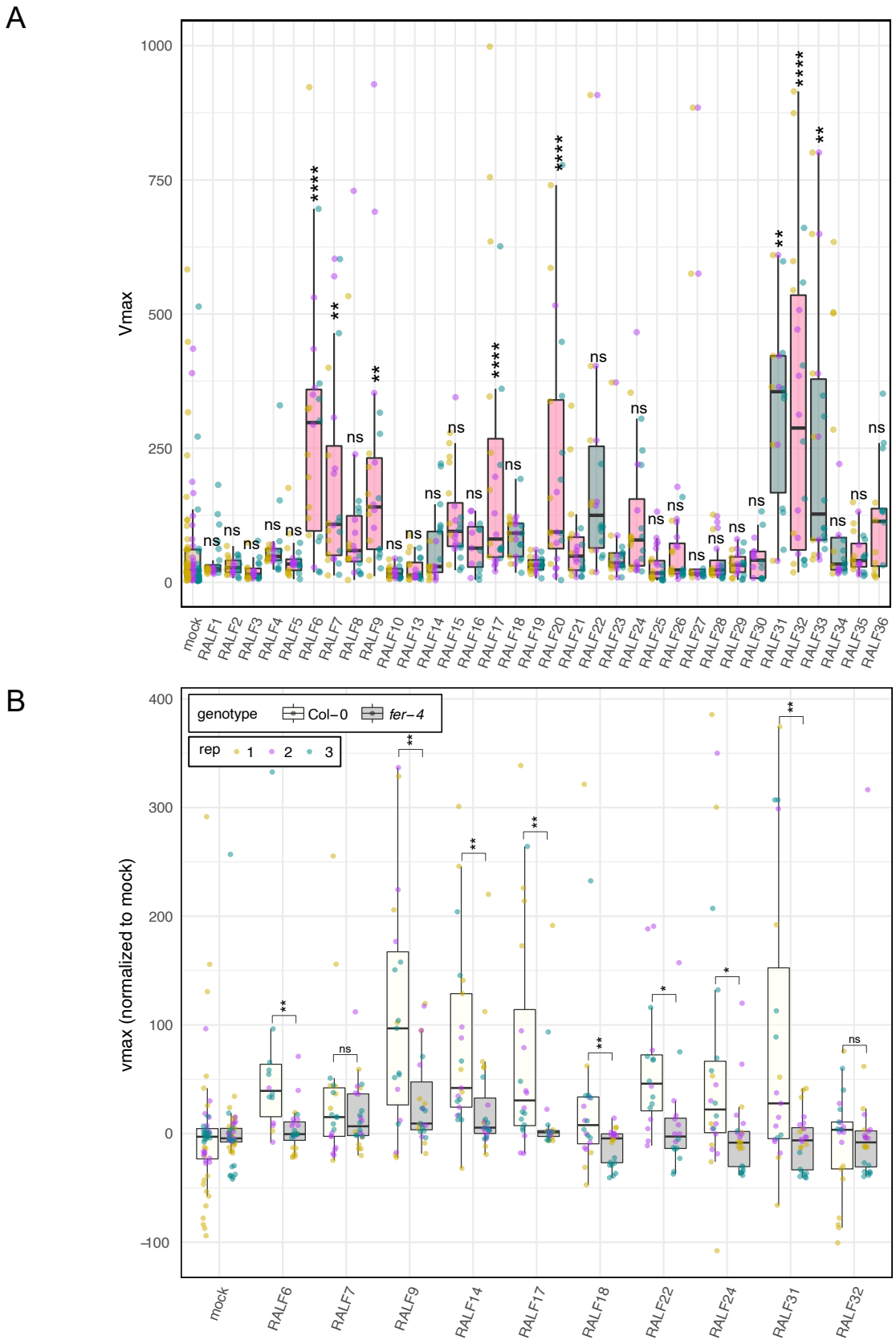

Supplemental Figure S10. Effect of predicted *At*RALF peptides on ROS production in Col-0 and *fer-4*. (A) ROS production in Col-0 leaf discs treated with 1 μM RALF peptides. In blue, box-plots of predicted S1P-cleaved RALF peptides and in pink, box plots of non-cleaved RALF peptides. Maximal velocity values of the ROS curves are shown, n = 8. Asterisks indicate significance levels of a one-way ANOVA followed by a Dunnet test comparing each treatment to mock. (B) ROS production in Col-0 and *fer-4* leaf discs treated with 1 μM RALF peptides (n=8). Col-0 data are shown in white and *fer-4* data in grey. Maximal velocity values of the ROS curves relative to mock data are shown, n = 8. Asterisks indicate significance levels of a two-tailed T-test comparing each treatment in *fer-4* to the corresponding in Col-0. A and B, Data from three independent repetitions are shown (colours indicate different replicates). Upper and lower whiskers represent 1.5 times and −1.5 times interquartile range; upper and lower hinges represent 25 % and 75 % quartiles; middle represents median or 50 % quartile. Asterisk significance: ns (p-value >0.05), ** (p-value ≤ 0.01), *** (p-value ≤ 0.001) and **** (p-value ≤ 0.0001).

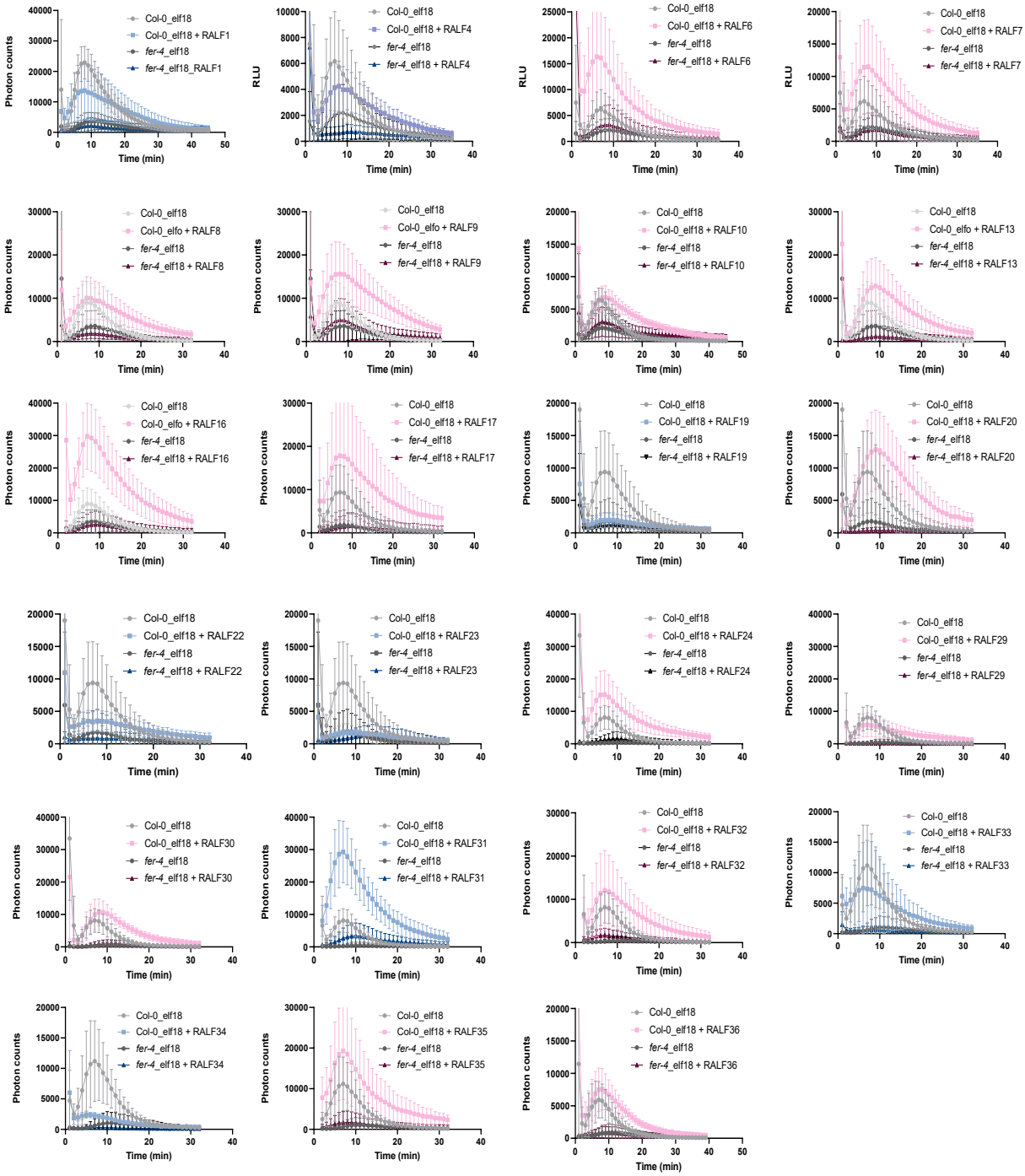

Supplemental Figure S11. FER-dependency of *At*RALF peptide effects on elf18-induced ROS production. ROS production in Col-0 and *fer-4* leaf discs co-treated with 100 nM elf18 and 1 µM RALF peptides or elf18 alone as control. Shown are the kinetics of one representative replicate. Predicted S1P-cleaved RALF peptides are indicated in blue and non-cleaved in pink.

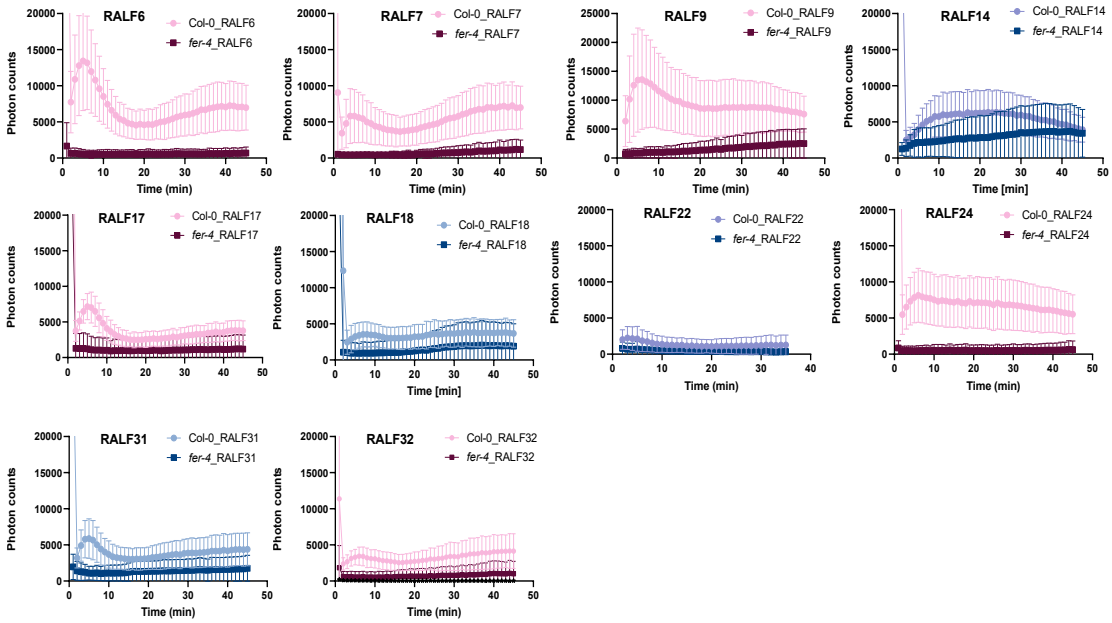

Supplemental Figure S12. FER-dependency of *At*RALF peptide effects on ROS production. ROS production in Col-0 and *fer-4* leaf discs treated with 1 μM RALF peptides. Shown are the kinetics of one representative replicate. Predicted S1P-cleaved RALF peptides are indicated in blue and non-cleaved in pink.

Supplemental Table S1. Re-annotation of *At*RALFs. Literature comparison of the *At*RALF peptide annotation used in different publications (listed in chronological order) and databases. Pink rows indicate inconsistency in the annotation and the final column coloured in green shows our proposed consensus *At*RALF annotation.

ATG number	TAIR	Protein accession	Olsen et al.,2002	Cao and Shi et al., 2012	Haruta et al., 2014	Morato do Canto et al., 2014	Stegmann et al., 2017	Campbell & Turner et al.,2017	Consensus
AT1G02900	RALF1	Q9SRY3	RALF1	AT1G02900	RALF1	RALF1	RALF1	AT1G02900	RALF1
AT1G23145	RALF2	A8MQ92	RALF2	AT1G23145	RALF2	RALF2	RALF2	AT1G23145	RALF2
AT1G23147	RALF3	A7REE5	RALF3	AT1G23147	RALF3	RALF3	RALF3	AT1G23147	RALF3
AT1G28270	RALF4	Q6TF26	RALF4	AT1G28270	RALF4	RALF4	RALF4	AT1G28270	RALF4
AT1G35467	RALF5	A8MQI8	RALF5	AT1G35467	RALF5	RALF5	RALF5	AT1G35467	RALF5
AT1G60625	RALF6	A8MQM2	RALF6	AT1G60625	RALF6	RALF6	RALF6	AT1G60625	RALF6
AT1G60815	RALF7	A8MRD4	RALF7	AT1G60815	RALF7	RALF7	RALF7	AT1G60815	RALF7
AT1G61563	RALF8	Q1ECR9	RALF8	AT1G61563	RALF8	RALF8	RALF8	AT1G61563	RALF8
AT1G61566	RALF9	Q3ECL0	RALF9	AT1G61566	RALF9	RALF9	RALF9	AT1G61566	RALF9
AT2G19020	RALF10	O65919	RALF10	AT2G19020	RALF10	RALF10	RALF10	AT2G19020	RALF10
AT2G19030	RALF11	O64466	RALF11	AT2G19030	RALF11	RALF11	RALF11	AT2G19030	RALF11
AT2G19040	RALF12	F4ISE1	RALF12	AT2G19040	RALF12	RALF12	RALF12	AT2G19040	RALF12
AT2G19045	RALF13	F4ISE2	RALF13	AT2G19045	RALF13	RALF13	RALF13	AT2G19045	RALF13
AT2G20660	RALF14	Q9SIU6	RALF14	AT2G20660	RALF14	RALF14	RALF14	AT2G20660	RALF14
AT2G22055	RALF15	A8MQM7	RALF15	AT2G22055	RALF15	RALF15	RALF15	AT2G22055	RALF15
AT2G32835	RALF16	A8MRM1	RALF16	AT2G32835	RALF16	RALF16	RALF16	AT2G32835	RALF16
AT2G32885	RALF36	A8MR00	-	AT2G32885	-	RALF17	RALF17	AT2G32885	RALF17
AT2G32890	RALF17	O48776	RALF17	-	RALF17	-	-	AT2G32890	AT2G32890
AT2G33130	RALF18	O49320	RALF18	AT2G33130	RALF18	RALF18	RALF18	AT2G33130	RALF18
AT2G33775	RALF19	Q6NME6	RALF19	AT2G33775	RALF19	RALF19	RALF19	AT2G33775	RALF19
AT2G34825	RALF20	A8MQL7	RALF20	AT2G34825	RALF20	RALF20	RALF20	AT2G34825	RALF20
AT3G04735	RALF21	A8MRF9	RALF21	AT3G04735	RALF21	RALF21	RALF21	AT3G04735	RALF21
AT3G05490	RALF22	Q9MA62	RALF22	AT3G05490	RALF22	RALF22	RALF22	AT3G05490	RALF22
AT3G16570	RALF23	Q9LUS7	RALF23	AT3G16570	RALF23	RALF23	RALF23	AT3G16570	RALF23
AT3G23805	RALF24	Q9LK37	RALF24	AT3G23805	RALF24	RALF24	RALF24	AT3G23805	RALF24
AT3G25165	RALF25	Q9LSG0	RALF25	AT3G25165	RALF25	RALF25	RALF25	AT3G25165	RALF25
AT3G25170	RALF26	Q0V822	RALF26	AT3G25170	RALF26	RALF26	RALF26	AT3G25170	RALF26
AT3G29780	RALF27	Q9LH43	RALF27	-	RALF27	RALF27	RALF27	AT3G29780	RALF27
AT4G11510	RALF28	Q9LDU1	RALF28	AT4G11510	RALF28	RALF28	RALF28	AT4G11510	RALF28
AT4G11653	RALF29	A8MQP2	RALF29	AT4G11653	RALF29	RALF29	RALF29	AT4G11653	RALF29
AT4G13075	RALF30	A7REH2	RALF30	AT4G13075	RALF30	RALF30	RALF30	AT4G13075	RALF30
AT4G13950	RALF31	Q2HIM9	RALF31	AT4G13950	RALF31	RALF31	RALF31	AT4G13950	RALF31
AT4G14010	RALF32	O23262	RALF32	AT4G14010	RALF32	RALF32	RALF32	AT4G14010	RALF32
AT4G15800	RALF33	Q8L9P8	RALF33	AT4G15800	RALF33	RALF33	RALF33	AT4G15800	RALF33
AT5G67070	RALF34	Q9FHA6	RALF34	AT5G67070	RALF34	RALF34	RALF34	AT5G67070	RALF34
AT1G60913	-	A8MRK3	-	-	-	RALF35	RALF35	AT1G60913	RALF35
AT4G14020	-	O23263	-	AT4G14020	RALF35	-	-	AT4G14020	AT4G14020
AT2G32785	-	A8MR74	-	-	-	RALF36	RALF36	-	RALF36
AT2G32788	-	A8MRN0	-	-	-	RALF37	RALF37	-	RALF37

Supplemental Table S2. Sequences of *At*RALF peptides synthesized. Amino acid sequence of the synthesized RALF peptides.

Peptide	Sequence of synthesized RALF
RALF1	ATTKYISYQSLKRNSVPCSRRGASYYNCQNGAQANPYSRGCSKIARCRS
RALF2	AQKVIGYPAIGRDGARGCSPKDPSCPQQPEKPYKRGCEKITRCERDRRKQAHLRNPRKVLDVVAVMAKAKQLY
RALF3	GYPKQRFGEDRTNPYEEITPPLIGGCDPKNPQTCLPKQPANPYRRGCLKITRCQRDV
RALF4	ARGRRYIGYDALKKNNVPCSRRGRSYYDCKKRRRNNPYRRGCSAITHCYRYAR
RALF5	AKRYIEYPPWQKHPCNPRFPTPDCYKRTPANPYRRGCTCISRCRRDCGGLSTWKKLLDTILKIPV
RALF6	QTYINYNGMKGDIIPGCSSKNPKECVKIPAYSYNRGCEISTRCQRQQHSSSS
RALF7	IKQINYKDLIKDTIPGCTSKNPKECVKVPANTYHRGCEISTRCHREQHSSSG
RALF8	SVRYITYPAIDRGDHAVHCDKAHPNTCKKKQANPYRRGCGVLEGCHRETGPKPT
RALF9	TRYITYPAIDRGDHAVHCDKAHPNTCKKKEANPYQRGCEKINRCRGG
RALF10	VPVESRRKHLDYGVITKCAGPNPPPGCYPPGAQQKNPTPANEYRRGCSKITRCKRD
RALF13	EPVESRNYIEYGAINKCAGPNPPPGCNPPGAEQKNPNPVNEYSRGCSKIHRCRRD
RALF14	QASRYISYEALKKNLPDNRRGEPDQRDNPYRRSCDVHSHCYRFTN
RALF15	TRYISYRGMNHGDHAIHCDKAHPNTCKKQVANPYRRGCGTIERCRRDTGRK
RALF16	RTLGYGSIKGDRIPACGYKNPNSCVKQPVNHYHRGCEKITRCARDAARYTESFNVDDDESPIINLH
RALF17	NSIGAPAMREDLPKGCAPGSSAGCKMQPANPYKPGCEASQRCRGG
RALF18	AKRFIDYEALKKNLPAKPDGKPDKPDNKYRRGCSAATGCYRFTN
RALF19	AARRSYISYGALRKNNVPCSRRGRSYYDCKKRKRANPYRRGCSVITHCYRQTS
RALF20	AKTIGNPAMREDEPKGCPPGSPASCKMQPANPYKPGCEASQRCRGT
RALF21	KVIGYPGLKPDLPCDHHRYPSACAPSEQPVNPYRRGCSKIHRCRRDSPPAPISRKMLIRGQLIYNNAYNAYIQYP
RALF22	AQKKYISYGAMRRNSVPCSRRGASYYNCQRGAQANPYSRGCSTITRCRR
RALF23	ATRRYISYGALRRNTIPCSRRGASYYNCRRGAQANPYSRGCSAITRCRRS
RALF24	MMRKQYISYETLRRDMVPCQKPGASYYACRSGQANAYNRGCSVITRCARDTNDIKT
RALF25	NDNKRKYLLLDPCLRPNAPPGCHRQPYKPRTPVNVYSRGCTTINRCRRVQNP
RALF26	KYLNPGVLDRCRGPNPPAGCHPHNSHHKPRVPVHNYSRGCSRITRCRRDA
RALF27	SYKTLQKQPTCDGRIAGNCIGTVNPKGATCTYYQRCKRAA
RALF28	NEIGYPGMGRGDRQPGCDHGNCPPDQPANPYHRGCEKSKRCRGPDPPALPRKMI
RALF29	AKRYIEYPIRLDLGKGCDPRFPTAACYKRTPANPYRRPCTTANRCRRSTSSTRVPSLKTFVEIPPM
RALF30	AGGGKFLNPGVLDPCLRPNPPPECQAPGSAGKPRERVNEYKVGCSKLTRCDRVG
RALF31	MAQKRYIGYETLRRDMVPCQKPGASYYDCRSGQANSYSRGCDTITRCARDTNDINT
RALF32	QAHKLSYGALRRNQPACDGGKRGESYSTQCLPPPSNPYSRGCSKHYRCGRDS
RALF33	ATTKYISYGALRRNTVPCSRRGASYYNCRRGAQANPYSRGCSAITRCRR
RALF34	YWRRTKYYISYGALSANRVPCPPRSGRSYYTHNCFRARGPVHPYSRGCSSITRCRR
AT2G32890	GAAADVSRGGCGGGDGSLGDDNERCVEAVKEDDDDDVDDVYKVINKMRIYA
$RALF1_{CCCC}$	ATTKYISYQSLKRNSVPASRRGASYYNAQNGAQANPYSRGASKIARARS
$RALF1_{I113A}$	ATTKYASYQSLKRNSVPCSRRGASYYNCQNGAQANPYSRGCSKIARCRS
$RALF23_{CCCC}$	ATRRYISYGALRRNTIPASRRGASYYNARRGAQANPYSRGASAITRARRS
$RALF23_{I113A}$	ATRRYASYGALRRNTIPCSRRGASYYNCRRGAQANPYSRGCSAITRCRRS

Supplemental Table S3. Accesion numbers of the proteins used in this study.

Protein name	Accesion number
RALF1	AT1G02900
RALF2	AT1G23145
RALF3	AT1G23147
RALF4	AT1G28270
RALF5	AT1G35467
RALF6	AT1G60625
RALF7	AT1G60815
RALF8	AT1G61563
RALF9	AT1G61566
RALF10	AT2G19020
RALF13	AT2G19045
RALF14	AT2G20660
RALF15	AT2G22055
RALF16	AT2G32835
RALF17	AT2G32885
RALF18	AT2G33130
RALF19	AT2G33775
RALF20	At2g34825
RALF21	At3g04735
RALF22	At3g05490
RALF23	At3g16570
RALF24	At3g23805
RALF25	At3g25165
RALF26	At3g25170
RALF27	At3g29780
RALF28	At4g11510
RALF29	At4g11653
RALF30	At4g13075
RALF31	At4g13950
RALF32	At4g14010
RALF33	At4g15800
RALF34	At5g67070
RALF35	AT1G60913
RALF36	AT2G32785
FERONIA	AT3G51550
LLG1	AT5G56170